Carbohydrate Polymers 83 (2011) 858–864

Contents lists available at ScienceDirect

Carbohydrate Polymers

journal homepage: www.elsevier.com/locate/carbpol

Fabrication of alginate/nanoTiO$_2$ needle composite scaffolds for tissue engineering applications

V.V. Divya Rani [a], Roshni Ramachandran [a], K.P. Chennazhi [a], H. Tamura [b], S.V. Nair [a], R. Jayakumar [a,*]

[a] Amrita Centre for Nanosciences and Molecular Medicine, Amrita Institute of Medical Sciences and Research Centre, Amrita Vishwa Vidyapeetham, Kochi 682041, Kerala, India
[b] Faculty of Chemistry, Materials and Bioengineering, Kansai University, Osaka 5648680, Japan

ARTICLE INFO

Article history:
Received 7 August 2010
Received in revised form 24 August 2010
Accepted 26 August 2010
Available online 28 September 2010

Keywords:
Alginate
Scaffolds
Nanocomposites
Osteogenesis
Tissue engineering

ABSTRACT

Alginate is a naturally occurring polymer that has been widely accepted as biodegradable and biocompatible material. Incorporation of nanoceramic will improve the capability of polymeric scaffold for tissue regeneration. Hence, in this study we fabricated a nanocomposite scaffold using alginate with nanoTiO$_2$ needles by lyophilization technique. The prepared nanocomposite scaffold was characterized using SEM, XRD, FTIR and TGA. In addition, swelling, degradation and biomineralization capability of the scaffold were also evaluated. The developed nanocomposite scaffolds showed well controlled swelling and degradation when compared to the control alginate scaffold. Cytocompatibility was assessed using MTT assay and cell attachment studies. Results indicated no sign of toxicity and cells were found to be attached to the pore walls offered by the scaffolds. These results suggested that the developed nanocomposite scaffold possess the prerequisites for tissue engineering application. Hence, alginate/nanoTiO$_2$ composite scaffold can be used as a better option for tissue regeneration.

1. Introduction

Three-dimensional macro-porous polymeric scaffolds are utilized in tissue engineering biological substitutes, where they provide the biomechanical support for the seeded cells until they are organised into a functional tissue (Su, He, & Li, 1997). In addition to matrix chemistry, the architecture of the scaffolds has a decisive effect on the developing tissue in culture (O'Regen & Gratzel, 1991). In weakly adhesive scaffolds, these parameters may shape the regenerating tissue and induce its differential functions. After transplantation, the architecture of the macro-porous scaffolds can control the extent of scaffold vascularisation and tissue ingrowth. Over the past decade nanoscale inorganic materials with specific structural features, such as nanotubes, nanofibers, and nanorods have attracted much attention because of their novel functional and size dependent properties. Among these, TiO$_2$ has been extensively studied due to its extensive applications such as photocatalysts, gas sensors, and biomaterials. TiO$_2$ nanoparticles have been recently proposed as attractive filler materials for biodegradable polymer matrices (Boccaccini et al., 2006; Dalby, McCloy, Robertson, Wilkinson, & Oreffo, 2006; Torres et al., 2007).

Natural polymers like alginate, chitin, and chitosan enhance osteogenesis. Therefore, it can be used as a bone substitute for bone repair and reconstruction (Majeti & Ravi Kumar, 2000). Alginate, derived from brown sea algae is a random anionic linear polymer consisting of varying ratios of α-L-guluronic acid (G) and β-D-mannuronic acid (M) units (Sutherland, 1991). It is soluble in aqueous solution at room temperature and form stable gels in presence of divalent cations, such as Ca^{2+}, Ba^{2+}, and Sr^{2+} (Honghe, 1997; Wang, Zhang, Konno, & Saito, 1993). Being a hydrophilic polymer, the alginate sponge is easily wettable, allowing more efficient penetration of cells into matrix. Unique properties of alginate, combined with its biocompatibility (Klock et al., 1997; Schmidt, Chung, Andrews, Spyratou, & Tirner, 1992) hydrophilicity and relatively low cost have made it an important polymer in pharmaceutical applications like wound dressings, (Doyle, Roth, Smith, Li, & Dunn, 1996) dental impression materials (Cook, 1986), and cell encapsulation (Chang, Hortelano, Tse, & Awrey, 1994; Wang et al., 1997). Alginate scaffolds have potential application in regeneration of many types of tissues. Hence in this study we are focusing on fabrication of 3D, open porous, interconnected network structure of alginate, with the incorporation of TiO$_2$ nanoneedles for tissue engineering applications in detail.

2. Materials and methods

2.1. Materials

Titanium plates were purchased from Jayon surgicals, Palakkad. NaOH, minimum essential medium (MEM), 3-(4,5-dimethyhiazol-2-yl)-2,5-diphenyltetrazolium bromide MTT, hydrochloric acid

* Corresponding author. Tel.: +91 484 2801234; fax: +91 484 2802020.
E-mail addresses: shantinair@aims.amrita.edu, nairshanti@gmail.com (S.V. Nair), rjayakumar@aims.amrita.edu, jayakumar77@yahoo.com (R. Jayakumar).

0144-8617/$ – see front matter © 2010 Elsevier Ltd. All rights reserved.
doi:10.1016/j.carbpol.2010.08.065

(HCl), Triton-X 100 and DAPI was purchased from Sigma–Aldrich, USA. Glutaraldehyde and hen lysozyme was purchased from Fluka. Trypsin–EDTA and foetal bovine serum (FBS) were obtained from Gibco Invitrogen Corporation. Alginate powder and was purchased from Sigma–Aldrich, USA.

2.2. Preparation of TiO_2 nanoneedles

For preparing TiO_2 nanoneedles commercially available titanium plates (14 mm^2 in diameter) were mechanically polished using 600 grit silicon carbide prior to the study. The samples were ultrasonically cleaned in acetone and distilled water before the hydrothermal process. The cleaned Ti plates were immersed in a 70 ml Teflon lined stainless steel autoclave containing 0.5 N NaOH and was subjected to hydrothermal treatment in a furnace. The temperature of the furnace was held constant at 250 °C using a programmable temperature controller for a period of 6 h (Divya Rani, Manzoor, Deepthy, Selvamurugan, & Nair, 2009). After the process the samples were taken out and ultra sonicated for 3 min to get the needles formed on the surface of the Ti plates into distilled water. The resultant TiO_2 nanoneedles in the solution were quantified by, taking 1 ml of the solution into a watch glass and then drying it, to take the weight of nanoneedles in 1 ml solution.

2.3. Preparation of alginate/nanoTiO_2 composite scaffolds

Alginate powder 2% (w/v) was taken and dissolved in distilled water under stirring condition till a clear homogenous solution was obtained. To obtain alginate nanoTiO_2 composite scaffold, 2% (w/v) TiO_2 nanoneedles were added to the solution and kept for stirring for 3 h till the nanoTiO_2 got completely mixed into the solution. After stirring, the resultant mixtures were transferred into a 12-well plate and pre freezed at −20 °C for 12 h. Then the frozen mixture was freeze dried (Christ alpha LD plus) at −80 °C for 24 h. Then the scaffolds were immersed in 2% $CaCl_2$ solution for 1 h and then again freeze dried for 24 h and then stored for further use.

2.4. Characterizations

The structural morphology of the composite scaffolds was examined using scanning electron microscope (SEM). Composite scaffold samples were prepared by taking a thin section of the scaffold using a razor blade. The section was then platinum sputter coated in vacuum (JEOL, JFC-1600, Japan), and examined using scanning electron microscope (JEOL, JSM-6490LA, Japan).

XRD patterns of the composite scaffolds were analyzed at room temperature using a Panalytical diffractometer (XPERT PRO powder) (Cu Kα radiations) operating at a voltage of 40 kV. XRD were taken 2θ angle range of 5–60° and the process parameters were: scan step size 0.02 and scan step time 0.05 s. TG studies were done

2.5. Swelling studies

The swelling studies were performed in PBS at pH 7.4 at 37 °C. The dry weight of the scaffold was noted (Wo). Scaffolds were placed in PBS buffer solution at pH 7.4 for7 days. The scaffolds were removed each day and the surface adsorbed water was removed by filter paper and wet weight was recorded (Ww). The ratio of swelling was determined using the following formula:

$$\text{Swelling ratio} = \frac{\text{Ww} - \text{Wo}}{\text{Wo}}$$

2.6. In vitro degradation studies

The degradation pattern of the composite scaffold was studied in PBS medium containing lysozyme at 37 °C. 6 groups of scaffolds (3 scaffolds in each) were immersed in lysozyme (10,000 μ/ml) containing PBS and incubated for up to 6 weeks. After each week one of the scaffolds was washed and in deionised water to remove ions adsorbed on the surface and were freeze dried. Initial weight of the scaffold was noted as Wo and dry weight as Wt. The degradation of scaffolds was calculated using the following formula:

$$\text{Degradation \%} = \frac{\text{Wo} - \text{Wt}}{\text{Wo}} \times 100$$

2.7. In vitro biomineralization studies

Three scaffolds of equal weight and shape was immersed in 1× simulated body fluid (SBF) (Kokubo & Takadama, 2006) solution and the incubated at 37 °C in closed falcon tube for 7 and 14 days. After the specified time, scaffolds were removed and washed three times with deionised water to remove adsorbed minerals. Finally the scaffolds were air dried at room temperature, sectioned and viewed using SEM for mineralization.

2.8. Cell culture studies

Cell studies were conducted using osteosarcoma cells (MG-63), Fibroblast cells (L-929) and human mesenchymal stem cells (hMSCs). Cell lines were maintained in the cell culture facilities with 10% FBS and 100 μl/ml penicillin–streptomycin. Cells were detached from the culture plate at 80–85% confluency and used for seeding on the scaffolds for investigating the cytocompatibility of the composite scaffolds. Prior to seeding of cells, scaffolds were sterilized with UV treatment and incubated with the culture medium for 1 h at 37 °C in a humidified incubator with 5% CO_2 and 85% humidity. Cells were seeded drop wise onto the scaffolds (1×10^5 cells/100 μl of medium/scaffold), which fully adsorbed the media, allowing cells to distribute throughout the scaffolds. Subsequently the cell seeded scaffolds were kept at 37 °C in a humidified incubator under standard culturing conditions for 4 h in order to allow the cells to attach to the scaffolds. After 4 h, the scaffolds were fed with additional culture medium and incubated for 48 h.

2.9. Cytocompatibility of the scaffolds

The viability of cells grown on the scaffolds was determined using the colorimetric MTT (3-(4,5-dimethylthiazol-2-yl)-2,5-diphenyltetrazolium bromide) assay. MTT assay measures the reduction of the tetrazolium component MTT by viable cells. Therefore, the level of the reduction of MTT into formazan can reflect the level of cell metabolism. For the assay, cells were then seeded on to 96-well plates at a density of 10^4 cells/well and were incubated under standard culturing conditions. Extract from the scaffolds were prepared by incubating the pre-sterilized scaffolds incubated in culture medium for 24 h and 48 h at 37 °C with agitation and the medium with leachables was collected in a falcon tube. Culture media of the seeded cells were replaced after 24 h by the extract (media with the leachables). Cells were incubated on the extract for 24 h. After the incubation period, fresh media containing 10% of MTT solution replaced the extract. Then the plates were incubated at 37 °C in humidified atmosphere for 4 h. Then the medium was removed, 100 μl of solubilisation buffer (Triton-X 100, 0.1N HCl and isopropanol) was added to each well to dissolve the formazan crystals. The absorbance of the lysate was measured in a micro plate reader (biotek) at a wavelength of 570 nm. Leachables

from chitin–chitosan scaffolds incubated in culture medium were used as positive control.

2.10. Cell morphology on the scaffolds

Morphology and spreading pattern of cells on the composite scaffolds were evaluated 48 h after seeding using SEM. For SEM analysis, cell seeded composite scaffolds were fixed with 2.5% glutaraldehyde, rinsed with PBS and dehydrated using graded series of ethanol (20–100%). The samples were coated with platinum and examined under SEM. Further DAPI staining was also done to study cell attachment on the scaffold. For DAPI analysis, cell seeded composite scaffolds were fixed with paraformaldehyde for 20 min, then washed with PBS and the 50 μl of DAPI (1:30 dilution) was added to each scaffold and incubated for 3 min. The scaffolds were then washed with PBS and observed under the microscope.

3. Results and discussions

3.1. Characterization

The prepared TiO_2 nanoneedles were characterized using SEM, EDAX and XRD. SEM image of TiO_2 is shown in Fig. 1a and b. The diameter of the nanoTiO_2 varied from 50 to 100 μm as measured by SEM. The XRD pattern of all the as-prepared nanostructured samples shown in Fig. 1c, revealed crystalline titania (TiO_2) containing a mixture of anatase and rutile phases. Energy dispersive X-ray spectrum (EDAX), displayed in Fig. 1d, confirmed that the surface exhibited mainly Ti peaks with only impurity levels of Na, which is probably from the residual Na after washing with water.

SEM images of the composite scaffolds showed that scaffolds were macro-porous in nature. No visible changes were seen in alginate and alginate/nanoTiO_2 composite scaffolds (Fig. 2a–d). The diameter of the nanoTiO_2 varied from 50 to 100 μm as measured by SEM. The pore size we obtained of the composite scaffold was in the range of 100–150 μm as compared to 150–200 μm in the control alginate scaffold. For tissue engineering scaffolds the ideal pore size range 150–200 μm as reported earlier (Bhatia, Yarmush, & Toner, 1997; Li et al., 2009) thus it can be said that the pore size of the composite scaffolds is ideal for tissue engineering applications. Thermal degradation of the scaffolds was studies using TG (Fig. 2e). We observed that there is a slower degradation rate prominent for the composite scaffolds compared to the control, which could be due to the incorporation of nanoceramics into them. We analyzed the degradation of both the scaffolds started from 100 °C and after 150 °C, a sudden decrease in weight was observed due to loss of moisture content. Between 350 and 500 °C there is a slight difference in weight loss, which confirms the slower degradation of nanocomposites when compared to conventional control scaffolds.

The XRD spectrum (Fig. 2f_a) of TiO_2 showed peaks at 25° (2θ). The XRD spectrum (Fig. 2f_b and f_c) of alginate gave a broad peak from 20° to 80° (2θ) due to its amorphous nature. The XRD of the composite however gave specific peaks at 25° corresponding to TiO_2. The sharp peaks we obtained here might be due to the overpowering crystallinity of titania.

3.2. Swelling studies

Swelling facilitates the infiltration of cells into the scaffolds in a three-dimensional fashion, during *in vitro* cell culture (as already proved by proved by Shanmugasundaram et al., 2001) where they suggest that desirable swelling and increase in pore size facilitates cell attachment and growth in a three-dimensional fashion. Increase in the pore size allows cells to avail the maximum internal

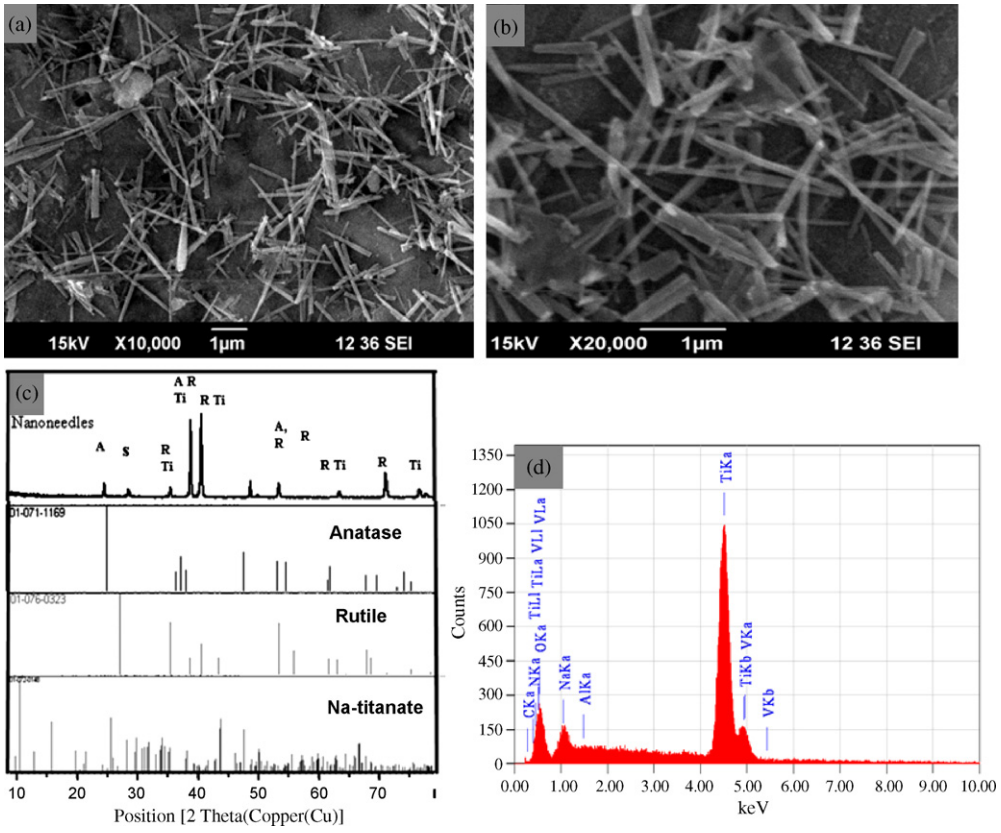

Fig. 1. (a and b) SEM image of TiO_2 nanoneedular structures synthesised by hydrothermal method, (c) XRD spectrum of nanoTiO_2 in comparison with JCPDS data of anatase, rutile and Na titantate, and (d) energy disperse spectrum of nanoTiO_2.

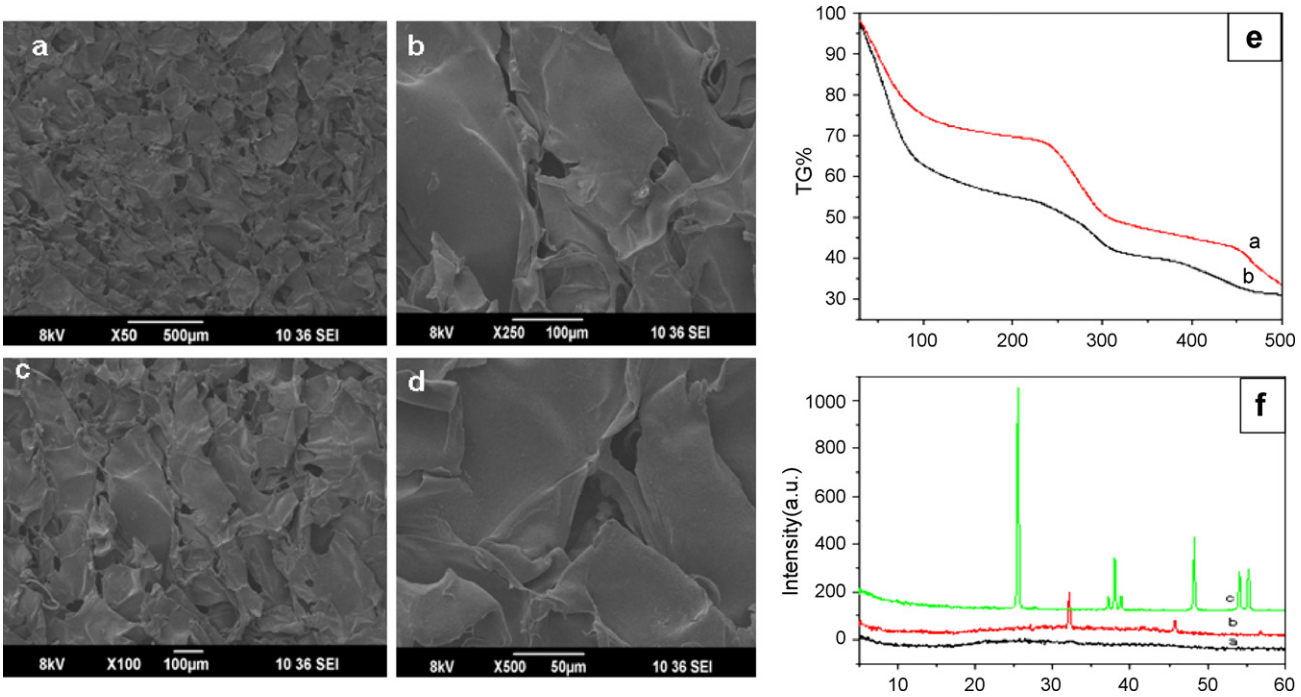

Fig. 2. SEM images of (a and b) alginate scaffolds, (c and d) alginate + TiO_2 scaffolds, (e) TG profiles of (a) alginate + TiO_2 and (b) alginate, and (f) XRD spectrum of (a) alginate, (b) alginate–nanoTiO_2 and (c) TiO_2.

surface of the scaffolds (Mikos et al., 1993; Zmora, Glicklis. & Cohen, 2002). Samples showing higher degree of swelling will have a larger surface area/volume ratio thus allowing the samples to have the maximum probability of cell growth in a three-dimensional fashion (Vacanti & Langer, 1999).

The increase in swelling also allows the samples to avail nutrients from culture media more effectively (Peter et al., 2009). However, increase in swelling will also decrease the mechanical properties of the scaffold. Hence, controlled swelling will be ideal for tissue engineering applications (Mikos et al., 1993). The incorporation of nanoTiO_2 decreased the swelling ability of nanocomposite scaffolds. This decrease in swelling rate with the addition of nanoTiO_2 may be due to their interaction with alginate network. Here in this study our results as in Fig. 3a show that the swelling rate of composite scaffolds can be controlled by adding nanoTiO_2.

3.3. In vitro degradation studies

Degradation of the scaffolds is very important parameter in tissue engineering. Ideally the scaffolds should degrade as new tissue formation takes place (Mikos et al., 1993; Vacanti & Langer, 1999). Here our study shows the *in vitro* degradation of chitin–chitosan, chitin–chitosan/nanoTiO_2 scaffolds, alginate and alginate/nanoTiO_2 after 4 weeks of immersion in PBS with lysozyme. Our results as in Fig. 3b show that the degradation rate was decreased with the addition nanoTiO_2 which may be due to the slow degradation property of TiO_2 present in the composite scaffolds.

3.4. In vitro biomineralization studies

A significant characteristic of a bioactive material is its ability to bond with living bone through the formation of an apatite interface layer on its surface both *in vitro* as well as *in vivo*. The bioactivity studies showed *in vitro* mineralization ability of the nanocomposite scaffolds. In our study, here the bioactivity studies of the chitin–chitosan/nanoTiO_2 and alginate/nanoTiO_2 nanocomposite scaffolds were performed in 1× SBF incubated for 7 and 14 days.

Fig. 4a–d shows the SEM images of an apatite like layer on the surface of alginate and alginate/nanoTiO_2 scaffolds. The XRD studies show sharp peaks corresponding to 32.6° (2θ) corresponding to hydroxyapatite layer on the scaffolds (Mikos et al., 1993) (Fig. 4e and f). The mineral deposits were seen to increase with time of incubation. After 14 days the deposit uniformly forms a layer on the surface. The bioactivity of the nanocomposite scaffolds allows for the formation of apatite layer, which results in direct bond-

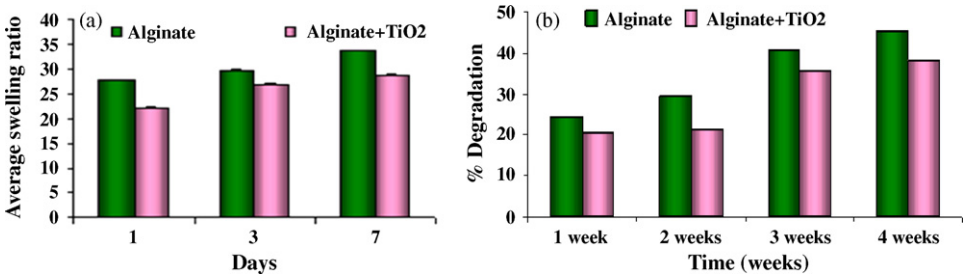

Fig. 3. Graph showing (a) swelling ratio of alginate and alginate/nanoTiO_2, and (b) percentage of degradation of alginate and alginate/nanoTiO_2.

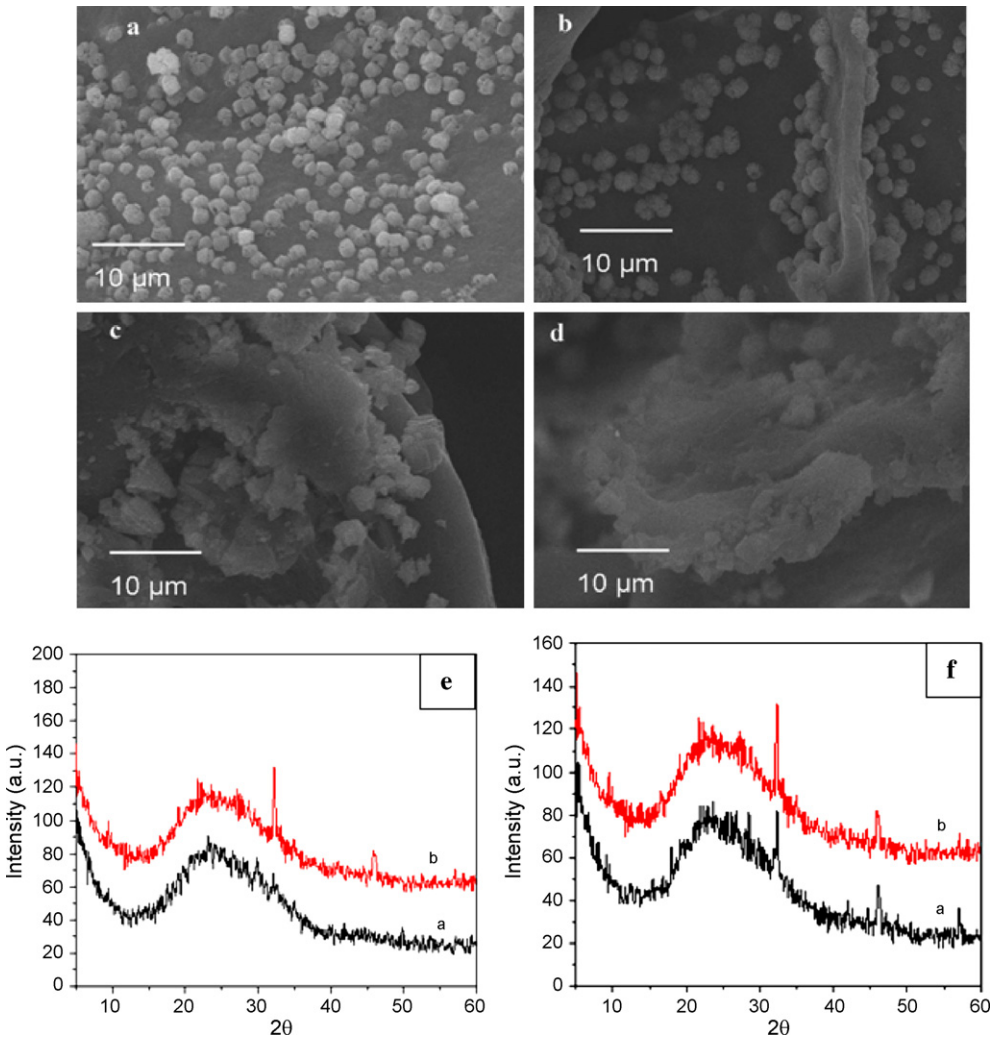

Fig. 4. SEM images of apatite formation on (a) alginate/nanoTiO$_2$ and (b) alginate after 7 days, (c) alginate/nanoTiO$_2$ and (d) alginate after 14 days in SBF solution. XRD spectrum of biomineralization, (e)—(a) alginate and (b) alginate/nanoTiO$_2$ after 7 days and (f)—(a) alginate and (b) alginate/nanoTiO$_2$ after 14 days.

ing of the implant with the bony defect. These results suggested that the nanocomposite scaffolds are a suitable material for tissue engineering applications.

3.5. Cytocompatibility studies

Alginate has already been proved to be a biocompatible polymer (Zmora et al., 2002). In this study we have assessed the cytocompatibility of the alginate/nanoTiO$_2$ was assessed using MTT assay similar to the above stated protocol. The results obtained showed no toxicity in the alginate/nanoTiO$_2$ nanocomposite scaffolds compared to the control alginate scaffolds (Fig. 5a and b). This result suggests that there are no significant toxic leachable in the alginate/nanoTiO$_2$ composite scaffolds compared to alginate scaffolds the control used as reference. The cell cytotoxicity was assessed by MTT assay and the results showed no significant cytotoxicity in the nanocomposite scaffolds. These results suggest that cell nanoTiO$_2$ is non-toxic to cells. The cytocompatibility of TiO$_2$ has already been proved earlier (Langer & Vacanti, 1993).

3.6. Cell attachment studies

SEM images was used to study the attachment, morphology and spreading of cells on the scaffolds. SEM images of cells incu-

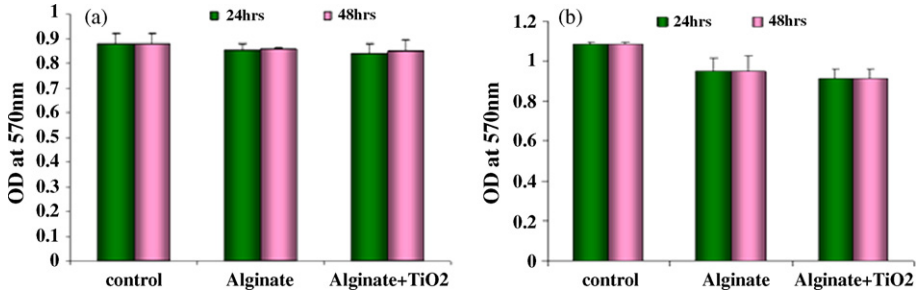

Fig. 5. MTT results of (a) alginate and alginate/nanoTiO$_2$ on MG-63 cells and (b) alginate and alginate/nanoTiO$_2$ on L-929 cells.

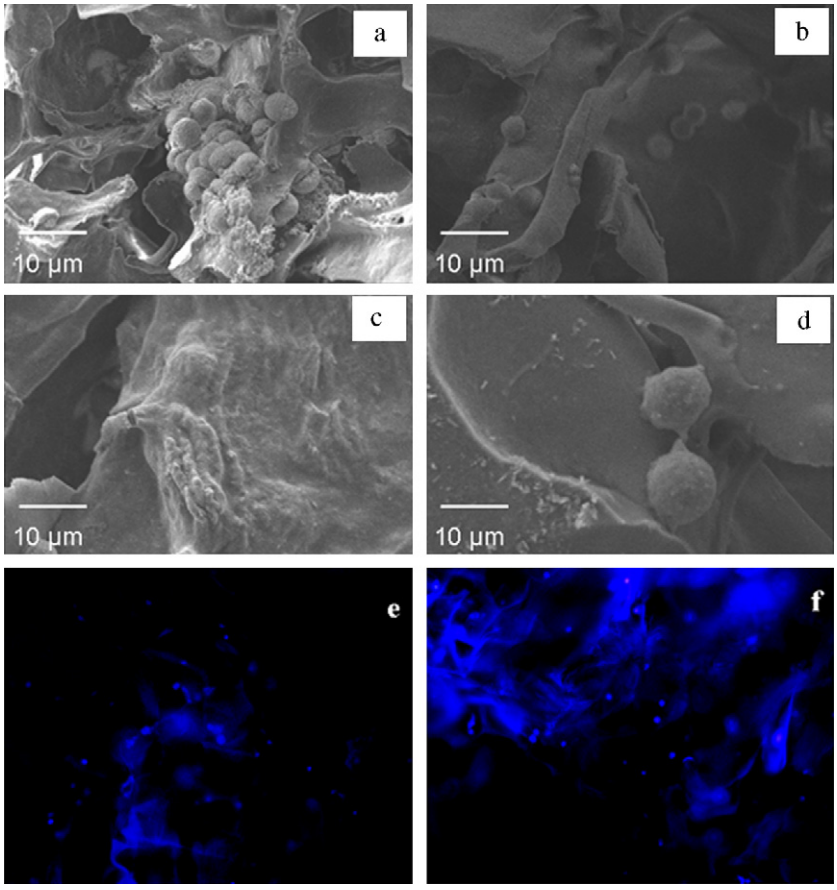

Fig. 6. SEM images showing cell attachment (MG-63) on (a and b) alginate, (c and d) alginate/nanoTiO$_2$ and DAPI staining on MG-63 cells attached on (e) alginate and (f) alginate/nanoTiO$_2$ scaffolds.

bated for 48 h on the scaffolds showed that cells attached and spread within the pore walls offered by the scaffolds. However, there were significant difference in morphology and spreading in a material dependent manner. After 48 h of incubation cells (MG-63 and L-929) on the control scaffolds remained in more or less round morphology (Fig. 6a and b).

In contrast, cells on the nanocomposite scaffolds exhibited a well spread morphology after the same period of incubation (Fig. 6c and d). Similar results were also obtained in case of L-929 cells as well. (Fig. 7a–d) Cell attachment studies showed that the nanocomposite scaffold significantly increased the cell attachment when compared to control scaffolds. The SEM images show flattened morphology

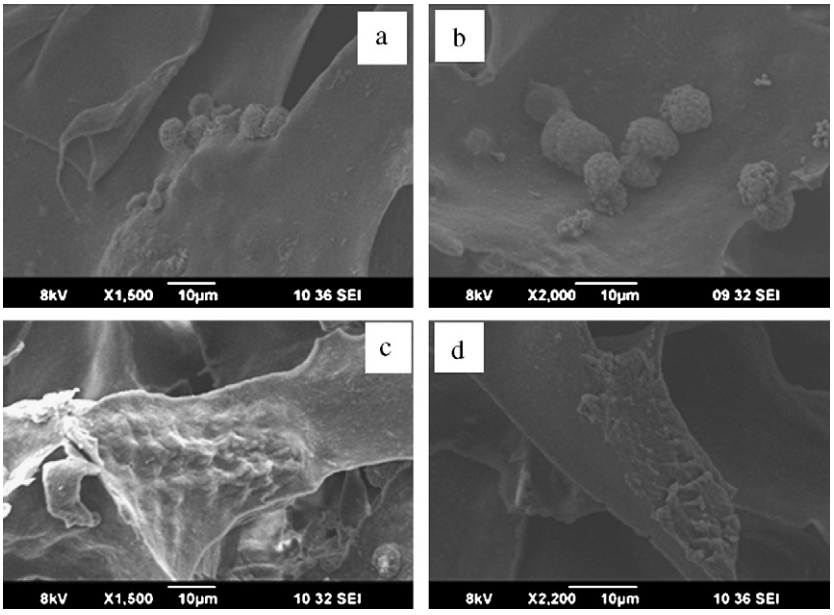

Fig. 7. SEM images showing cell attachment (L-929) on (a and b) alginate and (c and d) alginate/nanoTiO$_2$.

of MG-63 cells and forming bridges between pores. Previous works (Blaker, Gough, Maquet, Notingher, & Boccaccini, 2003; Langer & Vacanti, 1993) have shown similar results with MG-63 cell line. Similar results were obtained in L-929 cells. The result indicates that the nanocomposite scaffolds might be suitable for bone tissue engineering. The higher attachment on nanocomposite scaffolds may be due increase in surface area. It is known that surface topology could play a role in cell attachment on implants (Blaker et al., 2003; Hanawa, 1991). An increase in surface area allows maximum area for cell attachment and nano-surfaces have larger surface area to volume ratio. This larger surface area may play a role in increasing protein adsorption especially adhesive proteins. Further studies are needed to find out the specific protein adsorbed on the scaffold surface and their role cell attachment on nanocomposite scaffold. DAPI staining on the composite scaffolds (Fig. 6e and f).

4. Conclusions

The alginate/nanoTiO_2 composite scaffold was prepared and characterized for tissue engineering applications. The TGA studies showed slightly higher thermal stability than the conventional control scaffolds which can be attributed to the incorporated nanoceramics. These scaffolds showed adequate porosity, swelling, degradation and bioactivity properties required for efficient cell adhesion and proliferation in comparison to its control scaffolds. Cytotoxicity and cell attachment studies showed that the nanocomposites are non-toxic to an array of cell lines such as MG-63 and L-929 cells. These studies revealed that the prepared nanocomposite scaffold can be a better candidate for bone tissue regeneration.

Acknowledgements

The authors are thankful to the Department of Science and Technology, Government of India supported this work, under a centre grant of the Nanoscience and Nanotechnology Initiative program monitored by Dr. C.N.R. Rao. The authors are also thankful to Mr. Sajin P. Ravi for his help in SEM studies and Ms. Sreeja V. Nair for XRD analysis.

References

Bhatia, S. N., Yarmush, M. L., & Toner, M. (1997). Controlling cell interactions by micropatterning in co-cultures: Hepatocytes and 3T3 fibroblasts. *Journal of Biomedical Materials Research*, *34*, 189–199.

Blaker, J. J., Gough, J. E., Maquet, V., Notingher, I., & Boccaccini, A. R. (2003). In-vitro evaluation of novel bioactive composites based on Bioglass®-filled polylactide foams for bone tissue engineering scaffolds. *Journal of Biomedical Materials Research A*, *67*, 1401–1411.

Boccaccini, A. R., Blaker, J. J., Maquet, M., Chung, W., Jerome, R., & Nazhat, S. N. (2006). Poly (DL-lactide) (PDLLA) foams with TiO_2 nanoparticles and PDLLA/TiO_2—Bioglass foam composites for tissue engineering scaffolds. *Journal of Materials Science*, *41*, 3999–4008.

Chang, P. L., Hortelano, G., Tse, M., & Awrey, D. E. (1994). Growth of recombinant fibroblasts in alginate microcapsules. *Biotechnology & Bioengineering*, *43*, 925–932.

Cook, W. (1986). Alginate dental impression materials—Chemistry, structure, and properties. *Journal of Materials Science*, *20*, 1.

Dalby, M. J, McCloy, D., Robertson, M., Wilkinson, C. D. W., & Oreffo, R. C. (2006). Osteoprogenitor response to defined topographies with nanoscale depths. *Biomaterials*, *27*, 1306–1315.

Divya Rani, V. V., Manzoor, K., Deepthy, M., Selvamurugan, N., & Nair, S. V. (2009). The design of novel nanostructures on titanium by solution chemistry for an improved osteoblast response. *Nanotechnology*, *20*, 195101–195111.

Doyle, J. W., Roth, T. P., Smith, R. M., Li, Y., & Dunn, M. (1996). Effect of calcium alginate on cellular wound healing process modeled in vitro. *Journal of Materials Science*, *32*, 561–568.

Hanawa, T. (1991). In J. E. Davies (Ed.), *The Bone-Biomaterial Interface* (p. 49). University of Toronto Press.

Honghe. (1997). Interaction mechanism in sol–gel transition of alginate solutions by addition of divalent cations. *Journal of Carbohydrate Research*, *302*, 97–102.

Klock, G., Pfeffermann, A., Ryser, C., Grohn, P., Kuttler, B., Hahn, H. J., et al. (1997). Biocompatibility of mannuronic acid rich alginates. *Biomaterials*, *18*, 707–714.

Langer, R., & Vacanti, J. P. (1993). Tissue engineering. *Science*, *260*, 920–926.

Li, J., Dou, Y., Yang, J., Yin, Y., Zhang, H., Yao, F., et al. (2009). Surface characterization and biocompatibility of micro- and nano hydroxyapatite/chitosan–gelatin network films. *Material Science & Engineering C*, *29*, 1207–1215.

Majeti, N. V., & Ravi Kumar. (2000). A review of chitin and chitosan applications. *Reactive and Functional Polymer*, *46*, 1–27.

Mikos, A. G., Sarakinos, G., Lyman, M. D., Ingber, D. E., Vacanti, J. P., & Langer, R. (1993). Pre-vascularisation of porous biodegradable polymers. *Biotechnology and Bioengineering*, *42*, 716–723.

O'Regen, B., & Gratzel, M. (1991). A low-cost, high-efficiency solar cell based on dye sensitized colloidal TiO_2 films. *Nature*, *353*, 737–742.

Peter, M., Sudheesh Kumar, P. T., Binulal, N. S., Nair, S. V., Tamura, H., & Jayakumar, R. (2009). Development of novel chitin/nano bioactive glass ceramic nanocomposites scaffolds for tissue engineering applications. *Carbohydrate Polymers*, *78*, 926–931.

Schmidt, R. J., Chung, L. Y., Andrews, O., Spyratou, A. M., & Tirner, T. D. (1992). Biocompatibility of wound management products A study of the effects of various polysaccharides in murine L929 fibroblasts proliferation and macrophage respiratory burst. *Journal of Pharmaceutics and Pharmacology*, *45*, 508–516.

Shanmugasundaram, N., Ravichandran, P., Reddy, P. N., Ramamurty, N., Pal, S., & Rao, K. P. (2001). Collagen–chitosan polymeric scaffolds for the in vitro culture of human epidermoid carcinoma cells. *Biomaterials*, *22*(14), 1943–1951.

Su, B. T., He, Y. F., & Li, X. Y. (1997). Preparation and characterization of TiO_2/polymer complex nanomaterials. *Indian Journal of Chemistry B*, *36A*, 785.

Sutherland, I. W. (1991). *Novel materials from biological sources*. New York: Biomaterials Stockton Press., 309 pp.

Kokubo, T., & Takadama, H. (2006). How useful is SBF in predicting *in vivo* bone bioactivity. *Biomaterials*, *15*, 2907–2915.

Torres, F. G., Nazhat, S. N., Sheikh, M. D., Fadzullah, S. H., Maquet, M., & Boccaccini, A. R. (2007). Mechanical properties and bioactivity of porous PLGA/TiO_2 nanoparticle-filled composite for tissue engineering scaffolds. *Composite Science and Technology*, *67*, 1139–1147.

Vacanti, J. P., & Langer, R. (1999). Tissue engineering: the design and fabrication of living replacement devices for surgical reconstruction and transplantation. *Lancet*, *354*, 32–34.

Wang, T., Lacik, I., Brissova, M., Anilkumar, A. V., Prokop, A., Hunkler, D., et al. (1997). An encapsulation system for immunoisolation of pancreatic islets. *Nature Biotechnology*, *15*, 358–363.

Wang, Z., Zhang, Q., Konno, M., & Saito, S. (1993). Sol–gel transition of alginate solution by the addition of various divalent cations: ^{C}13-NMR spectroscopic study. *Biopolymers*, *33*, 703–706.

Zmora, S., Glicklis, R., & Cohen, S. (2002). Tailoring the pore architecture in 3-D scaffolds by controlling the freezing regime during fabrication. *Biomaterials*, *23*, 4087–4094.